Precise Measurement of the Neutron Skin Thicknesses of ^{208}Pb and ^{48}Ca

The PREX-II and CREX Experiments

Weibin Zhang
for the PREX/CREX collaboration

Stony Brook University
UC Riverside

February 7, 2023

Outline

Introduction

Questions

- What is the size of a heavy nucleus?
- What is the nuclear saturation density (ρ_0)?
- What is the symmetry energy (S_0) and its density dependence (L) at ρ_0?

Questions

- What is the size of a heavy nucleus?
- What is the nuclear saturation density (ρ_0)?
- What is the symmetry energy (S_0) and its density dependence (L) at ρ_0?

How ae neutrons arranged in atomic nuclei?

Neutron Skin Thickness

J. Phys. G: Nucl. Part. Phys. 46 (2019) 093003

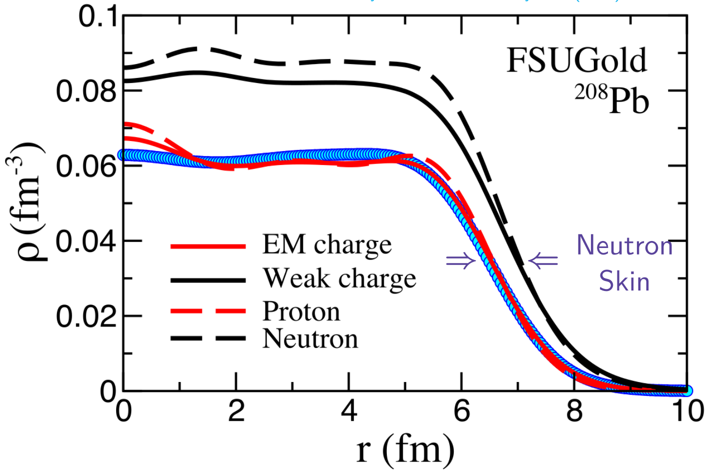

$$R_{p,n} \equiv \langle R_{p,n}^2 \rangle^{1/2} = \sqrt{\frac{\int d^3r\ \rho_{p,n}(r)\ r^2}{\int d^3r\ \rho_{p,n}(r)}} \qquad R_{\text{skin}} \equiv R_n - R_p$$

Equation of State (EOS)

Bethe-Weisäcker semi-empirical mass formula (liquid-drop model):

$$E = a_V A - a_S A^{2/3} - a_C \frac{Z(Z-1)}{A^{1/3}} - a_A \frac{(N-Z)^2}{A} + \frac{\delta a_p}{A^{3/4}}$$

Equation of State (EOS)

Bethe-Weisäcker semi-empirical mass formula (liquid-drop model):

$$E = a_V A - a_S A^{2/3} - a_C \frac{Z(Z-1)}{A^{1/3}} - a_A \frac{(N-Z)^2}{A} + \xcancel{\frac{\delta a_p}{A^{3/4}}}$$

Equation of State (EOS)

Bethe-Weisäcker semi-empirical mass formula (liquid-drop model):

$$E = a_V A - a_S A^{2/3} - a_C \frac{Z(Z-1)}{A^{1/3}} - a_A \frac{(N-Z)^2}{A} + \frac{\delta a_p}{A^{3/4}}$$

Equation of State (EOS)

Bethe-Weisäcker semi-empirical mass formula (liquid-drop model):

$$E = a_V A - \cancel{a_S A^{2/3}} - \xcancel{a_C \frac{Z(Z-1)}{A^{1/3}}} - a_A \frac{(N-Z)^2}{A} + \xcancel{\frac{\delta a_p}{A^{3/4}}}$$

Equation of State (EOS)

Bethe-Weisäcker semi-empirical mass formula (liquid-drop model):

$$E = a_V A - a_S A^{2/3} - a_C \frac{Z(Z-1)}{A^{1/3}} - a_A \frac{(N-Z)^2}{A} + \frac{\delta a_p}{A^{3/4}}$$

For infinite nuclear matter:

$$e = E/A \approx a_V - a_A \left(\frac{N-Z}{A} \right)^2$$

Equation of State (EOS)

Bethe-Weisäcker semi-empirical mass formula (liquid-drop model):

$$E = a_V A - \cancel{a_S A^{2/3}} - \xcancel{a_C \frac{Z(Z-1)}{A^{1/3}}} - a_A \frac{(N-Z)^2}{A} + \xcancel{\frac{\delta a_p}{A^{3/4}}}$$

For infinite nuclear matter:

$$e = E/A \approx a_V - a_A \left(\frac{N-Z}{A} \right)^2$$

$$e(\rho, \beta) = e(\rho, 0) + S(\rho)\beta^2 + O(\beta^4) \qquad \beta = \frac{\rho_n - \rho_p}{\rho_n + \rho_p}$$

Symmetry Energy

EOS:

$$e(\rho, \beta) = e(\rho, 0) + S(\rho)\beta^2 + O(\beta^4)$$

Symmetry energy:

$$S(\rho) = S(\rho_0) + \left.\frac{dS}{d\rho}\right|_{\rho_0} (\rho - \rho_0) + \frac{1}{2} \left.\frac{d^2S}{d\rho^2}\right|_{\rho_0} (\rho - \rho_0)^2 + \dots$$

$$S_0 = S(\rho_0) \qquad L = 3\rho_0 \left.\frac{dS}{d\rho}\right|_{\rho_0}$$

Neutron Stars

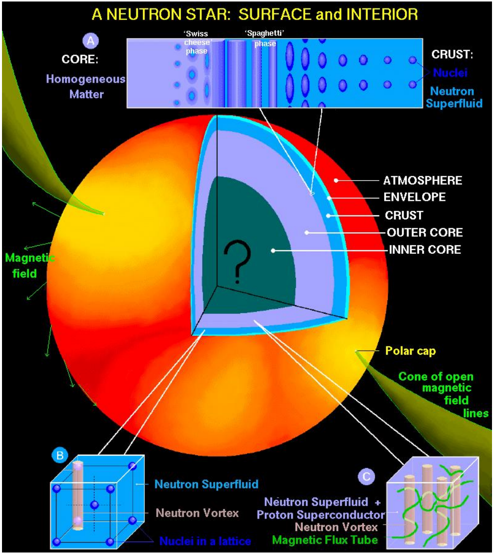

$$\beta \approx 1$$

$$e(\rho) \simeq e(\rho, 0) + S(\rho)$$

$$P = \rho^2 \frac{de}{d\rho} \simeq \rho^2 \frac{dS}{d\rho} = \frac{L(\rho)\rho}{3}$$

$$R_\star \simeq C(\rho, M) P^{0.23-0.26}$$

J. M. Lattimer and M. Prakash 2001 ApJ 550 426

Density Dependence of the Symmetry Energy

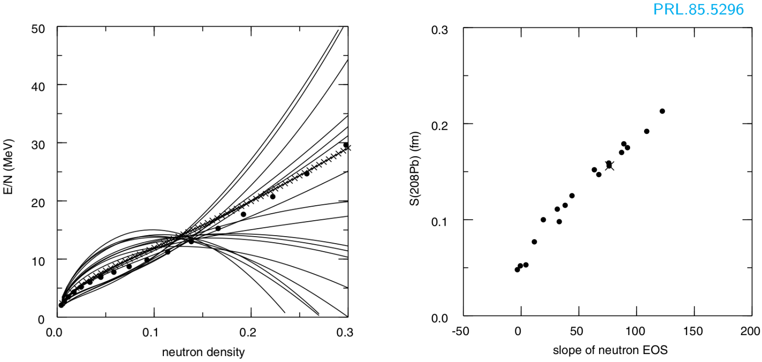

- L is poorly understood
- Precise measurement of the neutron skin thickness in ^{208}Pb can constrain L

Theoretical Predictions

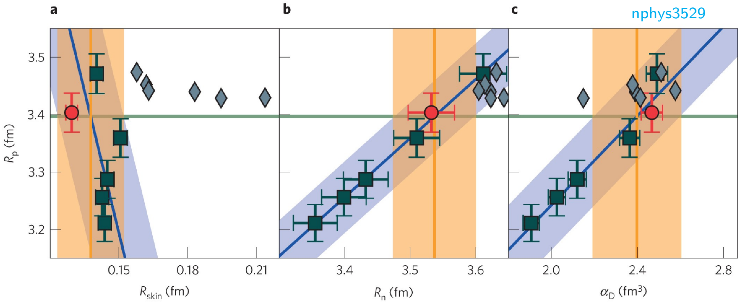

^{48}Ca

Eur. Phys. J. A (2014) 50: 48

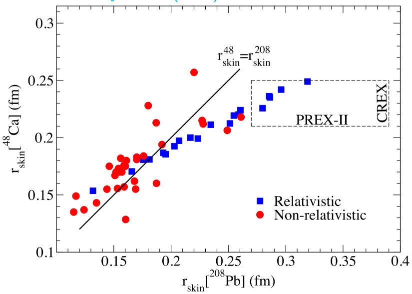

- Test microscopic models: ab-initio methods and the nuclear Density Functional Theory (DFT)
- Constrain three-nucleon force in ab-initio methods and isovector $(\rho_n - \rho_p)$ contribution in DFT

Parity-Violating Electron Scattering (PVES)

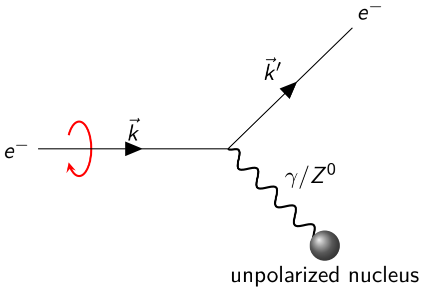

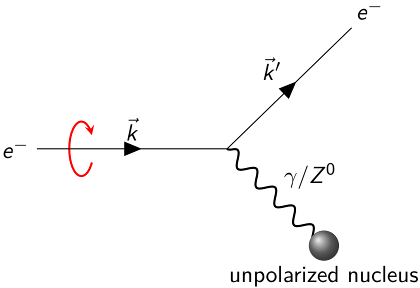

- Weak probe
- Interference with EM amplitude
- Clean, no QCD background as in hadronic probes
- Asymmetry is sensitive to the neutron distribution

	Electric charge	Weak charge
Proton	1	0.07
Neutron	0	-0.99

Asymmetry

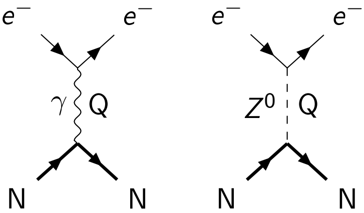

- γ interacts with only vector current
- Z^0 interacts with both vector and axial-vector currents

$$\mathcal{A}_{\mathrm{PV}} = \frac{\left(\frac{d\sigma}{d\Omega}\right)^R - \left(\frac{d\sigma}{d\Omega}\right)^L}{\left(\frac{d\sigma}{d\Omega}\right)^R + \left(\frac{d\sigma}{d\Omega}\right)^L} \approx \frac{G_F Q^2}{4\pi\alpha\sqrt{2}} \frac{Q_{wk}}{Z} \frac{F_{wk}(Q^2)}{F_{ch}(Q^2)} \sim 10^{-4} \frac{Q^2}{\mathrm{GeV}^2}$$

where:

$$F(Q^2) = \int d^3r \frac{sin(Qr)}{Qr} \rho(r)$$

- $\mathcal{A}_{\mathrm{PV}} \sim$ ppm, $\frac{\delta\mathcal{A}}{\mathcal{A}} \lesssim 4\% \Rightarrow \delta R_n \lesssim 0.05$ fm

Experimental Setup

Hall A at JLab

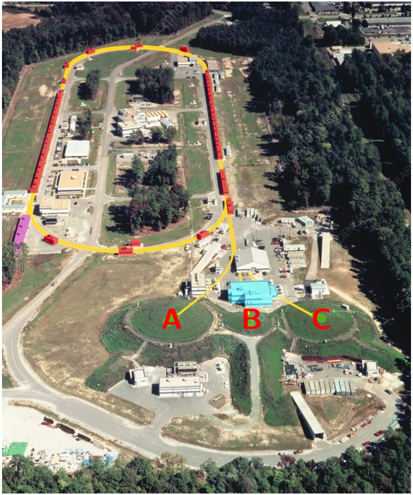

CEBAF

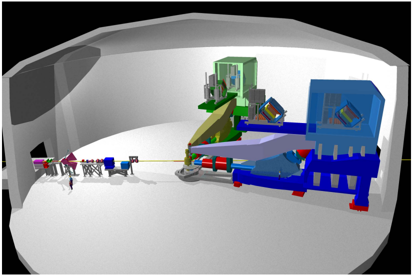

Hall A

	PREX-II	CREX
E (GeV)	0.95	2.18
θ (deg)	4.7	4.5

Polarized Electron Source: GaAs-Based Semiconductor

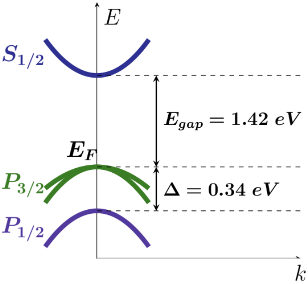

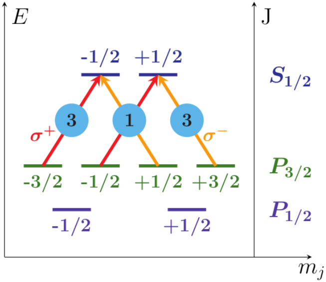

$$\mathcal{P} = \frac{3-1}{3+1} = 50\%$$

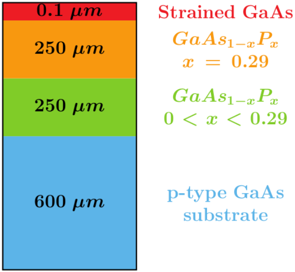

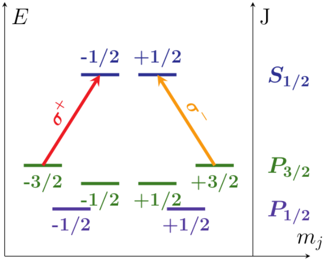

$$\mathcal{P} = 100\%$$

Helicity Control

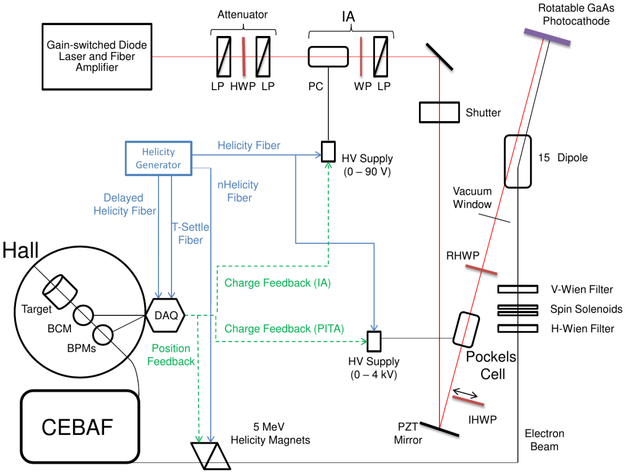

- Pockels Cell (PC): fast helicity flipping
- Insertable Half-Wave Plate (IHWP): slow helicty flipping
- Wien Filter: very slow helicity flipping

Polarimeters

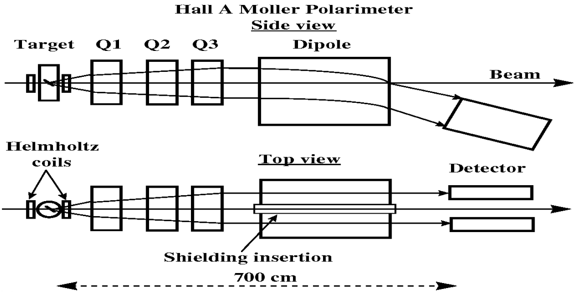

Hall A Møller polarimeter set-up

- Invasive, happens every few days
- PREX-II: $\mathcal{P} = (89.67 \pm 0.80)\%$
- CREX: $\mathcal{P} = (87.06 \pm 0.74)\%$

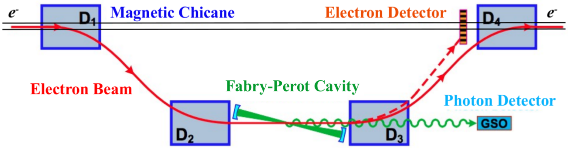

- Non-invasive
- PREX-II: $\mathcal{P} = (89.68 \pm 0.15)\%$
- CREX: $\mathcal{P} = (87.115 \pm 0.453)\%$

Septum and HRS

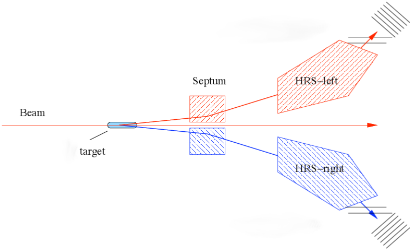

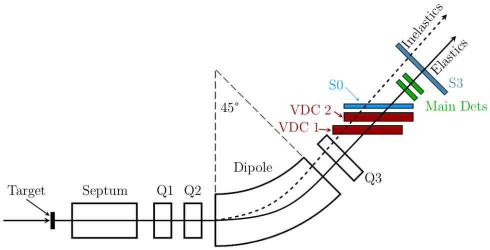

- Septum: make the small scattering angle of $\sim 5^\circ$ possible
- High Resolution Spectrometer (HRS): precise Q^2 measurement, reject inelastic scatterings

Detectors

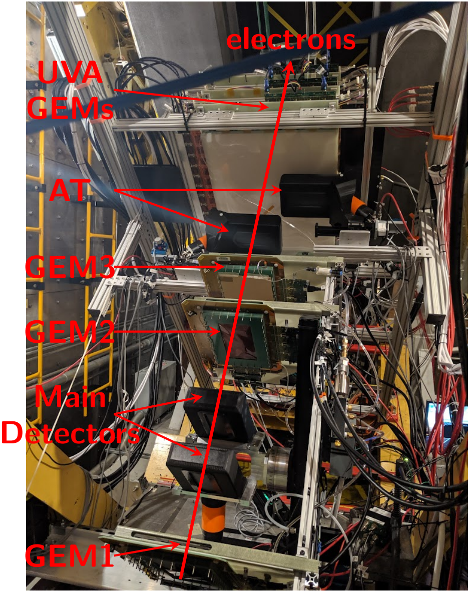

- Main Detectors: 5 mm thick fused silica (quartz) with a size of 16 cm long by 3.5 cm wide
- AT: also a quartz detector, used for monitoring the transverse polarization
- GEM: for optics study

Run Time

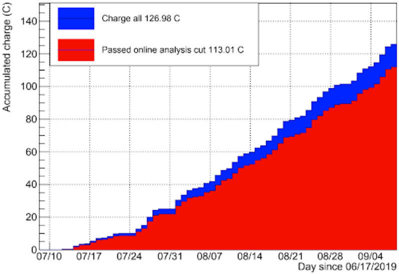

PREX-II: Jul - Sep, 2019

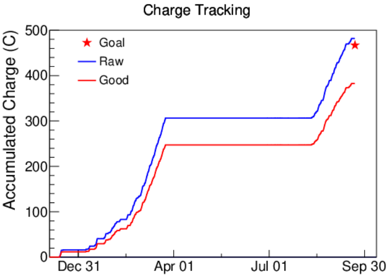

CREX: Dec, 2019 - Mar, 2020
Aug - Sep, 2020

Data Analysis

Asymmetry Extraction and Interpretation

$$\mathcal{A}_{\text{cor}} = \mathcal{A}_{\text{raw}} - \sum_i \beta_i \Delta x_i$$

$$\mathcal{A}_{\text{PV}} = \frac{\mathcal{A}_{\text{cor}}/\mathcal{P} - \sum_i \mathcal{A}_i f_i}{1 - \sum_i f_i}$$

- $\mathcal{A}_{\text{cor}}$: corrected asymmetry
- $\mathcal{A}_{\text{raw}}$: raw asymmetry
- β_i: correction coefficient
- Δx_i: beam fluctuation
- $\mathcal{P}$: beam polarization
- $\mathcal{A}_i$: background asymmetry
- f_i: background fraction

$$\langle \mathcal{A} \rangle = \frac{\int d\theta \sin\theta \mathcal{A}(\theta) \frac{d\sigma}{d\Omega} \epsilon(\theta)}{\int d\theta \sin\theta \frac{d\sigma}{d\Omega} \epsilon(\theta)}$$

- $\mathcal{A}(\theta)$: theoretical prediction
- $\epsilon(\theta)$: acceptance function

Raw Data ($\mathcal{A}_{\text{raw}}$)

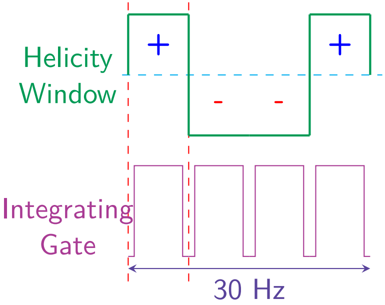

$$\mathcal{A}_{\text{raw}} = \frac{n^+ - n^-}{n^+ + n^-} + \mathcal{A}_{\text{blind}}$$
$$\approx \frac{N^+ - N^-}{N^+ + N^-} - \frac{I^+ - I^-}{I^+ + I^-} + \mathcal{A}_{\text{blind}}$$

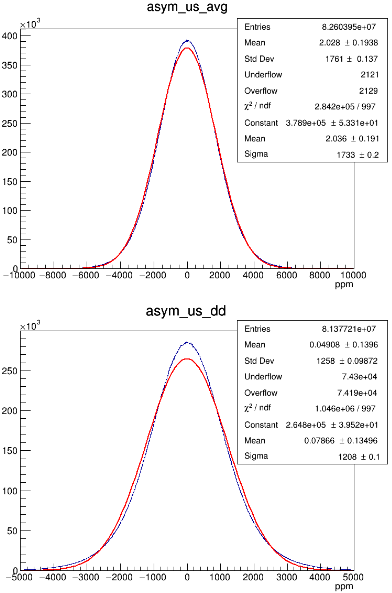

CREX raw asymmetry distributions

Helicity Correlated Beam Asymmetry (HCBA)

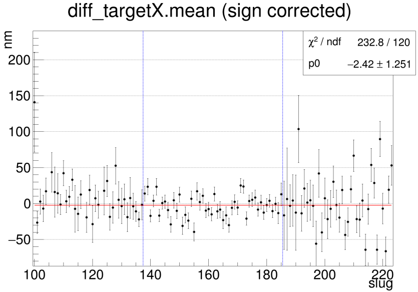

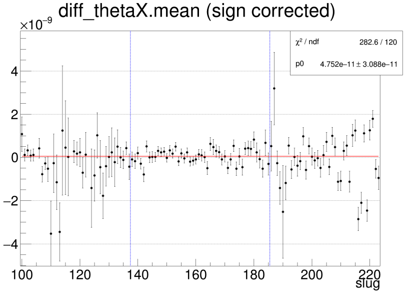

- False asymmetry caused by beam fluctuations
- Though of the fast helicity reversal, there is no way to eliminate beam flucatations completely

Regression

$$\mathcal{A}_{cor} = \mathcal{A}_{raw} - \sum_i \beta_{\mathbf{i}} \Delta x_i$$

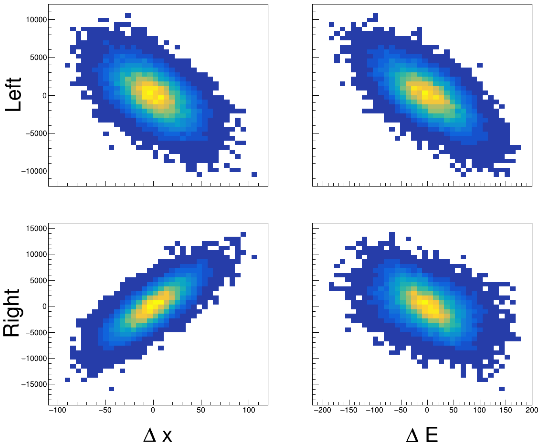

- Based on natural beam fluctuations, minimize the χ^2 of a given fit: $\chi^2 = \sum \left(\mathcal{A}_{raw} - \sum_i \beta_i \Delta M_i \right)^2 \quad \frac{\partial \chi^2}{\partial \beta_i} = 0$

Beam Modulation $\mathcal{A}_{\mathrm{cor}} = \mathcal{A}_{\mathrm{raw}} - \sum_i \beta_{\mathbf{i}} \Delta x_i$

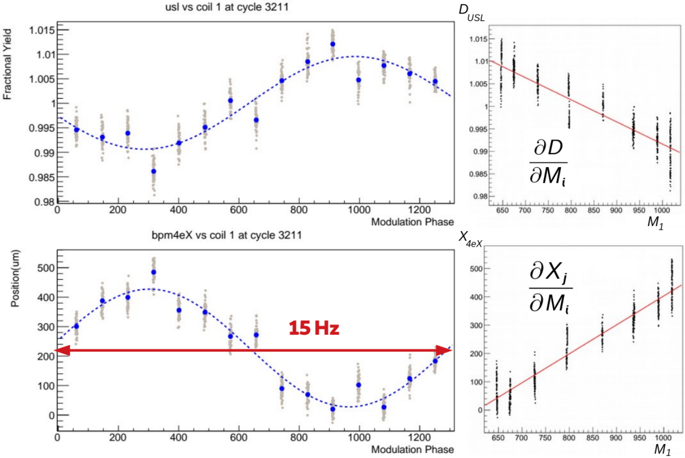

- Modulate the beam deliberately, and then measure the detector (monitor) response: $\frac{\partial D}{\partial C_j} = \sum_i^{N_{bpm}} \beta_i \frac{\partial M_i}{\partial C_j}$ $\quad \beta_i = \frac{\partial D}{\partial M_i}$

Lagrangian Multiplier

$\mathcal{A}_{\text{cor}} = \mathcal{A}_{\text{raw}} - \sum_i \beta_{\mathbf{i}} \Delta x_i$

$$\mathcal{L} = \chi^2 + \sum_i \lambda_i \left(\sum_j \frac{\partial D}{\partial C_j} \frac{\partial C_j}{\partial M_i} - \frac{\partial D}{\partial M_i} \right)$$

$$\frac{\partial \mathcal{L}}{\partial \beta} = 0 \qquad \frac{\partial \mathcal{L}}{\partial \lambda} = 0$$

- Regression is susceptible to instrumental noise
- Dithering is accurate, but not precise, limited by the low modulation frequency
- Lagrangian multiplier: try to combine these 2 techniques to avoid their drawbacks, while keeping their advantages

Corrected Asymmetry ($\mathcal{A}_{cor}$)

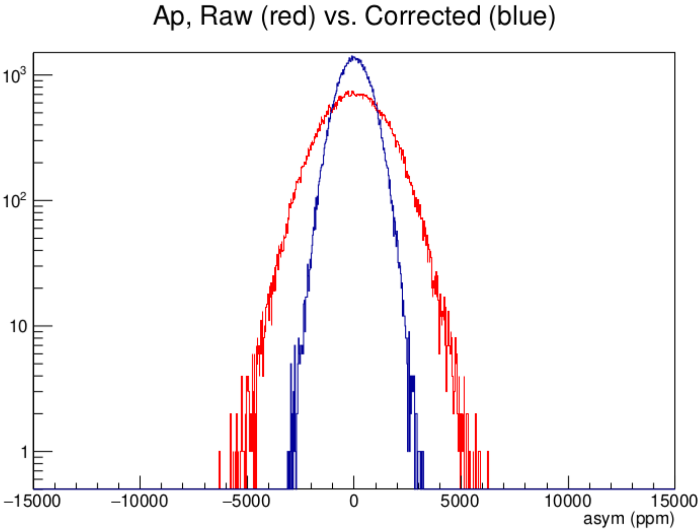

Comparison Between the Three Methods

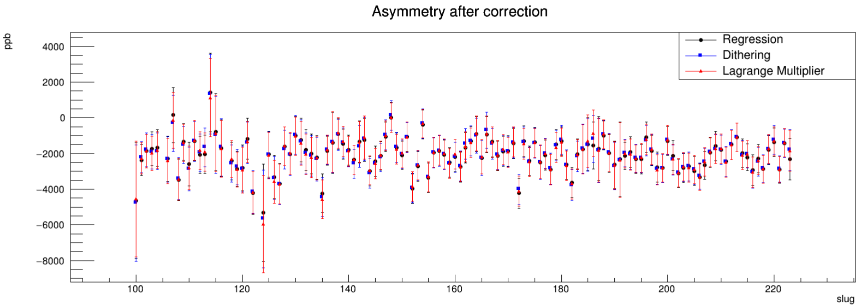

- Good agreement between the three methods
- Asymmetries corrected with the Lagrangian Multiplier are used

Result and Discussion

Final Number: $\mathcal{A}_{\mathbf{PV}}$

$$\mathcal{A}_{\text{cor}} = \mathcal{A}_{\text{raw}} - \sum_i \beta_i \Delta x_i$$

$$\mathcal{A}_{\text{PV}} = \frac{\mathcal{A}_{\text{cor}}/\mathcal{P} - \sum_i \mathcal{A}_i f_i}{1 - \sum_i f_i}$$

$\mathcal{A}$ (ppb)	PREX-II	CREX
$\mathcal{A}_{\text{raw}}$	431.64 ± 44.01	2106 ± 178.9
$\mathcal{A}_{\text{cor}}$	492.02 ± 13.52	2080.3 ± 83.8
$\mathcal{A}_{\text{PV}}$	$549.4 \pm 16.1_{\text{stat}} \pm 8.1_{\text{syst}}$	$2412.3 \pm 106.1_{\text{stat}} \pm 38.7_{\text{syst}}$
Unblinded $\mathcal{A}_{\text{PV}}$	$550.0 \pm 16_{\text{stat}} \pm 8_{\text{syst}}$	$2668 \pm 106_{\text{stat}} \pm 40_{\text{syst}}$

Final Number: R_{skin}

PRL 126, 172502

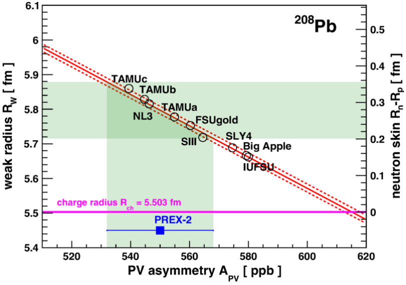

Exp	PREX-II	CREX
Target	^{208}Pb	^{48}Ca
$\langle Q^2 \rangle$ (GeV^2)	0.00616 ± 0.00005	0.0297 ± 0.0002
$\langle A_{PV} \rangle$ (ppb)	$550 \pm 16_{stat} \pm 8_{syst}$	$2668 \pm 106_{stat} \pm 40_{syst}$
F_W	$0.368 \pm 0.013_{exp} \pm 0.001_{theo}$	$0.1304 \pm 0.0052_{stat} \pm 0.0020_{syst}$
$F_{ch} - F_W$	$0.041 \pm 0.013_{exp} \pm 0.001_{theo}$	$0.0277 \pm 0.0052_{stat} \pm 0.0020_{syst}$
R_W (fm)	$5.795 \pm 0.082_{exp} \pm 0.013_{theo}$	$3.640 \pm 0.026_{exp} \pm 0.023_{theo}$
$R_n - R_p$ (fm)	$0.278 \pm 0.078_{exp} \pm 0.012_{theo}$	$0.121 \pm 0.026_{exp} \pm 0.024_{theo}$

Final Number: L

PRL 126, 172503

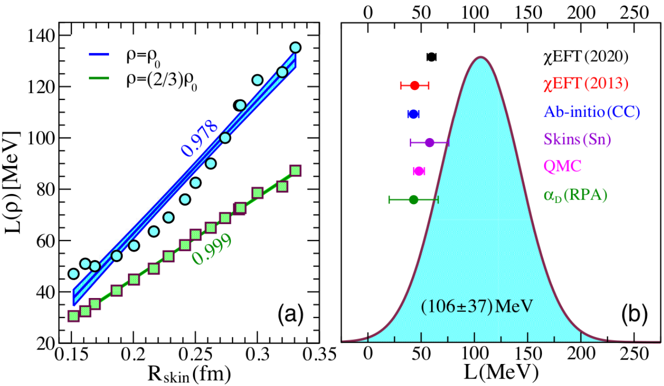

$$L(\rho_0) = 106 \pm 37 \text{ MeV} \qquad L(\rho_1) = 71.5 \pm 22.6 \text{ MeV}$$

Physical Implications: Nuclear Theory

PRL 129, 042501

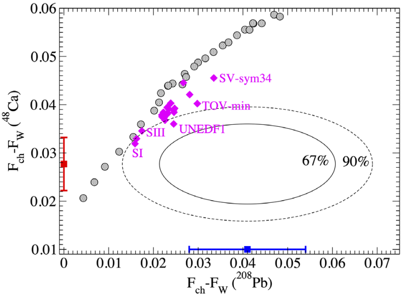

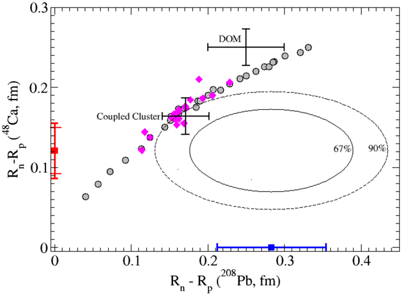

- Our results will guide the development of nulcear theories
- Only a few models' predictions match with both measurements simultaneously
- More work, from both experimental and theoretical sides, are needed to accommodate the difference between them

Physical Implications: Nuclear Saturation Density

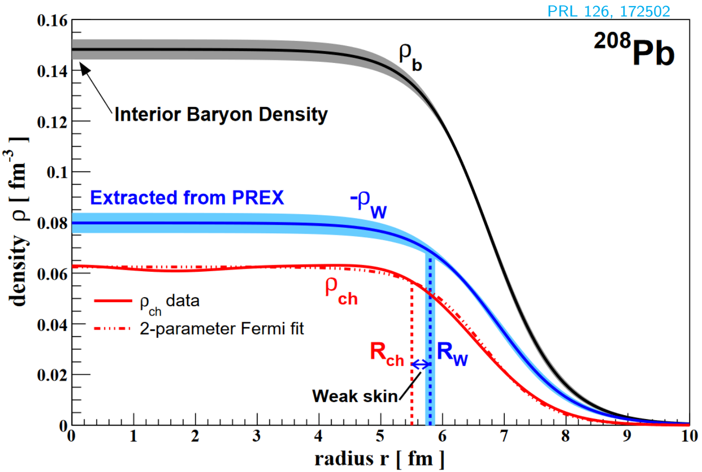

- Interior baryon density: $\rho_b = 0.1482 \pm 0.0040\ \mathrm{fm}^{-3}$
- Nuclear saturation density: $\rho_0 = 0.1510 \pm 0.0059\ \mathrm{fm}^{-3}$

Physical Implications: Size of a Neutron Star

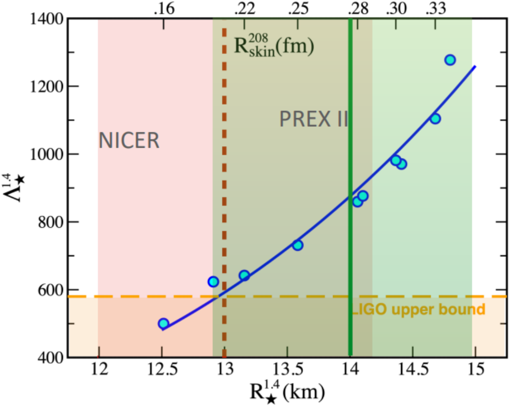

PREX-II result

- supports a large neutron star radius
- is consistent with the NICER result
- is in mild tension with the LIGO observation

Physical Implications: The Direct Ucra Process in Neutron Stars

PRL 126, 172503

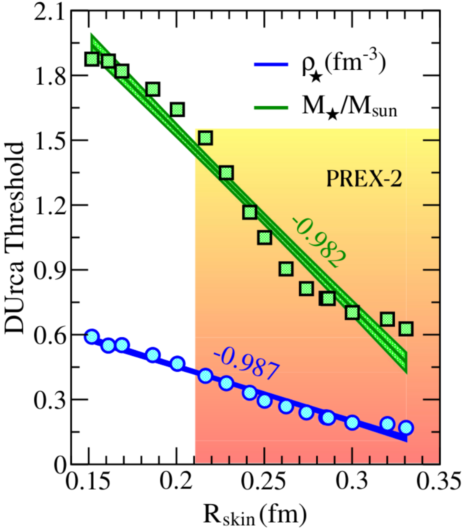

- PREX-II R_{skin} supports a lower threshold density:

$$\rho_\star \approx 0.24\ \mathrm{fm}^{-3}$$
$$M_\star \approx 0.85 M_\odot$$

Transverse Asymmetry

Introduction

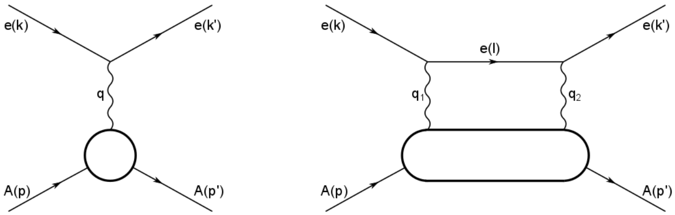

Transverse Asymmetry (Beam Normal Single Spin Asymmetry):

$$A_n = \frac{\sigma_\uparrow - \sigma_\downarrow}{\sigma_\uparrow + \sigma_\downarrow} \approx 0 + \frac{2\mathrm{Im}(T_{2\gamma} \cdot T_{1\gamma}^*)}{|T_{1\gamma}|^2}$$

- A_n is 0 under Born approximation
- A_n is sensitive to Two Photon Exchange (TPE) interaction
- A_n is a systematic uncertainty in the A_{PV} measurement for PREX-II/CREX

How to Measure Transverse Asymmetry

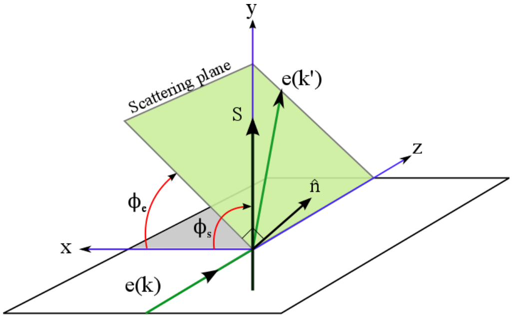

$$\mathcal{A}_{\text{meas}}(\phi_e) = \mathcal{A}_n(\vec{S}_e \cdot \hat{n}) = \mathcal{A}_n|\vec{S}_e|\sin(\phi_e - \phi_s)$$

- $\hat{n} \equiv \frac{(\vec{k}\times\vec{k}')}{|\vec{k}\times\vec{k}'|}$: normal direction of the scattering plane
- Azimuthal angle (ϕ_e) dependent
- Choose ϕ_s to be: 0° (horizontal) or 90° (**vertical**)

AT Result

PRL 128, 142501

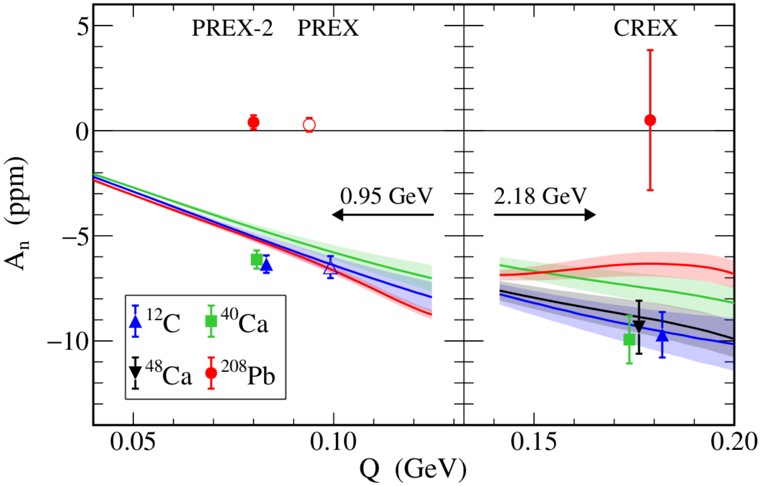

- A_n for Pb208 is consistanly 0 at a different Q^2 values
- First measurement of a new nucleus: Ca40

Summary

Parity Violating Asymmetry measurement

- Precise measurements of the neutron skin thicknesses of Pb208 and Ca48 (the first time)
- Both measurements are statistics limited
- **Constrain nuclear models and the density dependence of the symmetry energy (L)**

Transverse Asymmetry measurement

- Theory calculations agree with measurements for light nuclei
- **Transverse asymmetry is found to be consistent with 0 for Pb208 at all Q**

Backup

One Data Point

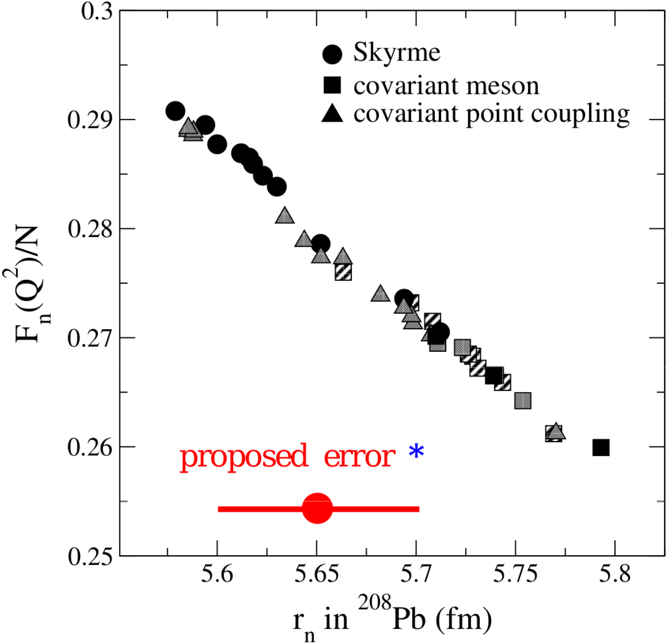

History of PVES

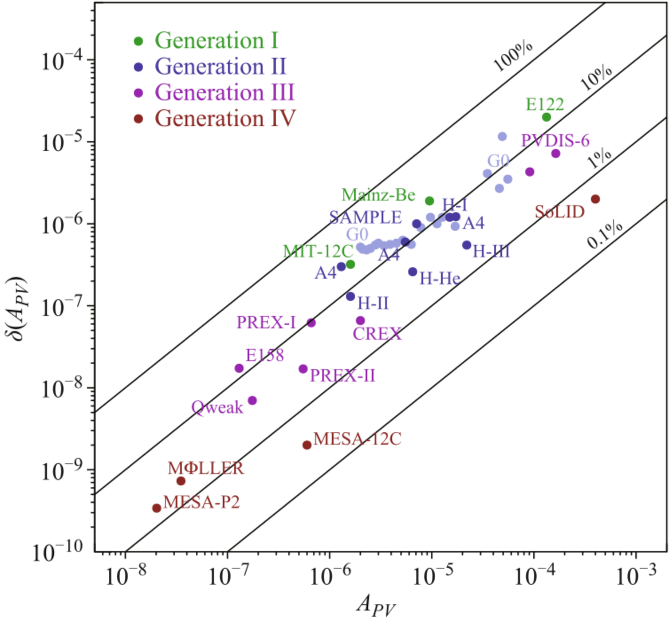

Why ^{208}Pb and ^{48}Ca?

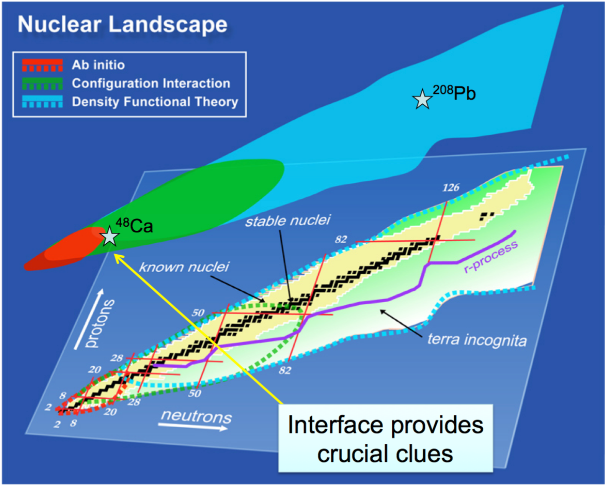

- Doubly magic nuclei
- Spin-0

Form Factors

$$\mathcal{A}_{\text{PV}} = \frac{\frac{d\sigma^R}{d\Omega} - \frac{d\sigma^L}{d\Omega}}{\frac{d\sigma^R}{d\Omega} + \frac{d\sigma^L}{d\Omega}} = \frac{|\mathcal{M}^R|^2 - |\mathcal{M}^L|^2}{|\mathcal{M}^R|^2 + |\mathcal{M}^L|^2}$$

$$\approx \frac{\mathcal{M}_Z^R - \mathcal{M}_Z^L}{\mathcal{M}_\gamma} \propto \frac{\frac{d\sigma_{\text{weak}}}{d\Omega}}{\frac{d\sigma_{\text{E+M}}}{d\Omega}} \qquad (\text{for low } Q^2)$$

$$\approx \frac{G_F Q^2}{4\pi\alpha\sqrt{2}} \frac{Q_{wk}}{Z} \frac{F_{wk}(Q^2)}{F_{ch}(Q^2)}$$

where: $\mathcal{M}^{R,L} = \mathcal{M}_\gamma + \mathcal{M}_Z^{R,L}$ $(\mathcal{M}_\gamma >> \mathcal{M}_Z)$ and

$$F(Q^2) = \int d^3r \frac{sin(Qr)}{Qr} \rho(r)$$

Dynamics

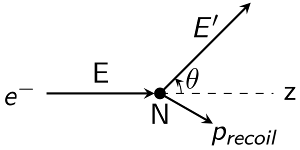

$$E' = \frac{ME}{M + E(1 - \cos\theta)}$$

where M is the mass of the target nucleus

- with very small scattering angle $\theta \sim 5^\circ$, $E' \approx E$, quasi-elastic scattering
- $Q^2 = -q^2 = -\left[(E - E')^2 - (\vec{p} - \vec{p}')^2\right] = 2EE'(1 - \cos\theta)$

Parameters

	PREX-II	CREX
Energy (GeV)	0.95	2.18
Beam current (μA)	50-85	100-150
Polarization (%)	89.7	87.1
Scattering angle θ (deg)	4.7	4.5
Q^2 (GeV^2)	0.00616	0.0297
Scattering rate (MHz/μA/arm)	$\sim$ 30	$\sim$ 0.2
Collected charge (C)	114	412

Figure-of-Merit (FOM)

$$\text{FOM} = R \times \mathcal{A}^2 \times \epsilon^2$$

- R: scattering rate
- $\mathcal{A}$: asymmetry
- $\epsilon = \frac{d\mathcal{A}/\mathcal{A}}{dR_n/R_n}$: sensitivity of the asymmetry w.r.t. neutron radius

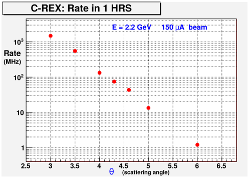

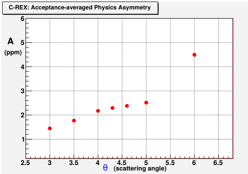

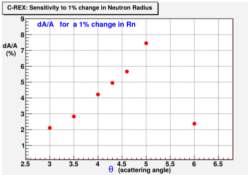

Asymmetry of ^{208}Pb

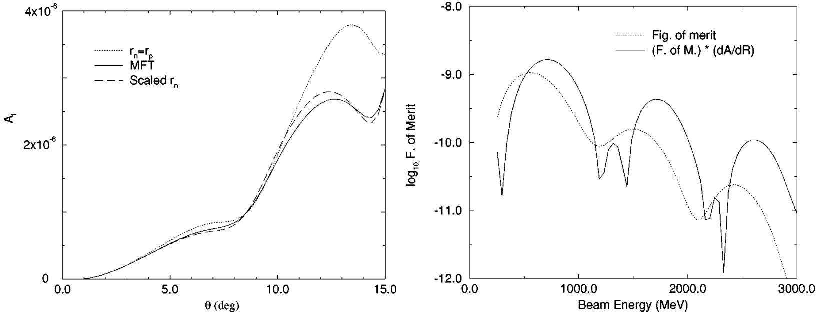

Figure: Parity-Violating asymmetry for ^{208}Pb. Left: E = 850 *GeV*; Right: $\theta = 6\,\mathrm{deg}$

Neutron Skin Thickness of ^{48}Ca

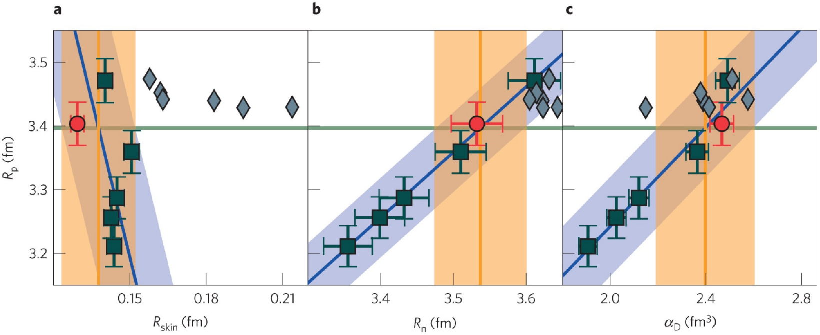

Figure: Ab-initio calculation of the neutron skin thickness of ^{48}Ca. From left to right, neutron skin thickness (a), neutron radius (b) and electric dipole polarizability (c) of ^{48}Ca are plotted versus its proton radius. The ab-initio predictions are shown as red circles and dark squares, while DFT results are represented by gray diamonds. The blue line represents a linear fit to ab-initio predictions. The horizontal green line marks the experimental value of R_p, whose intersection with the blue line.
nphys3529

Neutron Skin Thickness of ^{208}Pb

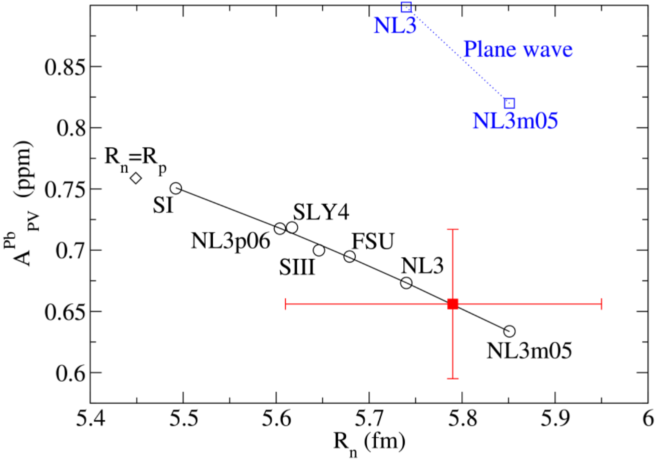

Figure: PREX-I result (red square). PhysRevLett.108.112502

CEBAF

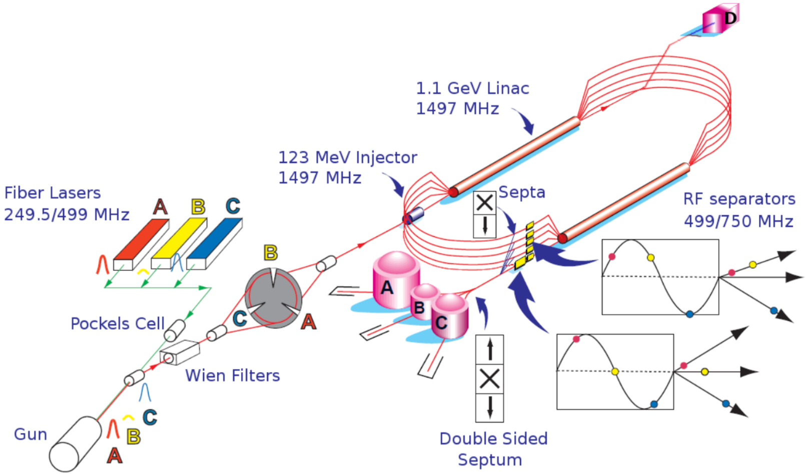

D
1.1 GeV Linac
1497 MHz
123 MeV Injector
1497 MHz
Septa
RF separators
499/750 MHz
Fiber Lasers
249.5/499 MHz
A
B
C
B
C
A
A
B
C
Pockels Cell
Wien Filters
Gun
C
B
A
Double Sided
Septum

Beamline

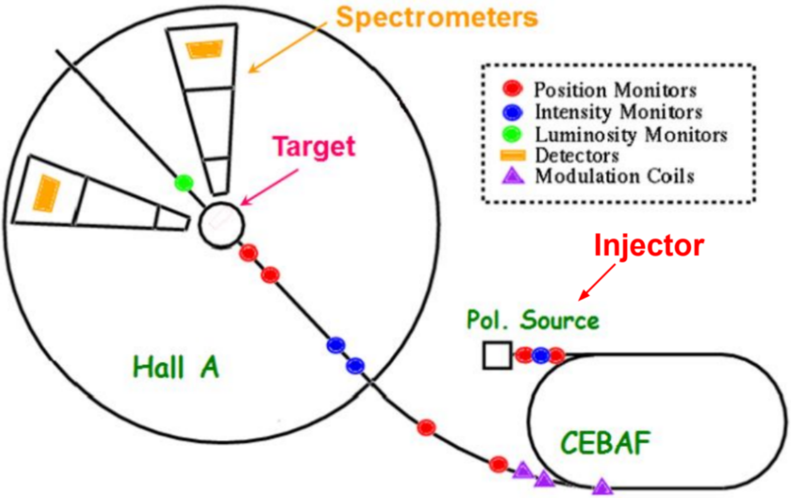
Spectrometers
Position Monitors
Intensity Monitors
Luminosity Monitors
Detectors
Modulation Coils
Target
Injector
Pol. Source
Hall A
CEBAF

Target Chamber

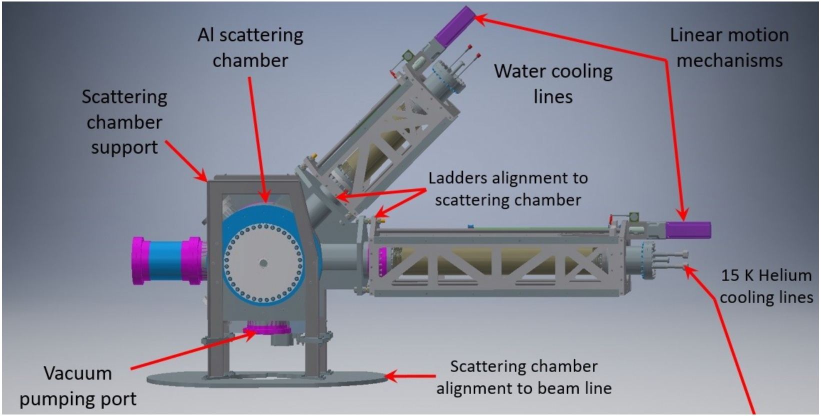

Pulsar Lightcurve

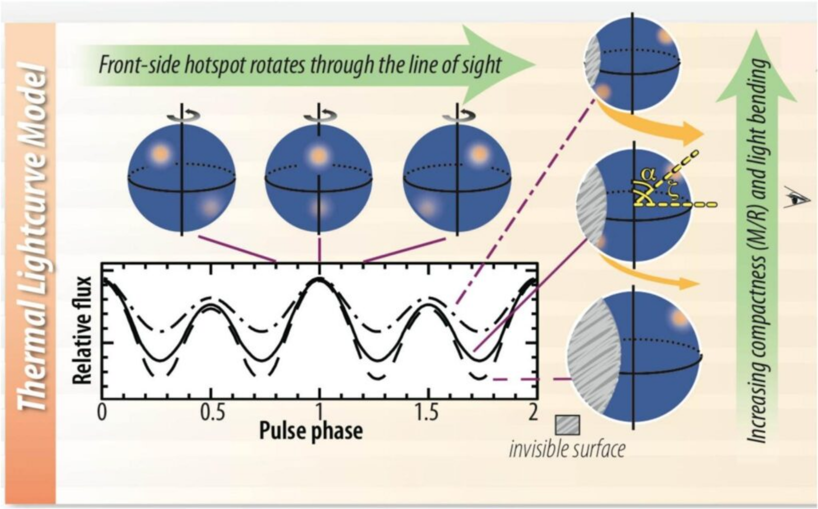

Scattering Theory

For scattering:

$$S = 1 + i(2\pi)^4\delta^{(4)}(\sum p_i - \sum p_f)T$$

The unitarity condition requires ($SS^\dagger = 1$):

$$T_{if} - T_{if}^\dagger = ia_{if}$$

Where a_{if} is the absorptive part of the amplitude T_{if}

$$a_{if} = \sum_\Gamma T_{i\Gamma} T_{\Gamma f}^\dagger (2\pi)^4\delta^{(4)}(\sum p_i - \sum p_\Gamma)$$

T-odd Effect[1]

Define time reverse operation (spin and momenta reversed):

$$\tilde{\Psi} = \mathcal{T}\Psi_{\uparrow}(\vec{k}) = \Psi_{\downarrow}(-\vec{k})$$

- Time reversal invariance: $|T_{if}|^2 = |T_{\tilde{f}\tilde{i}}|^2$
- T-odd: $\propto |T_{if}|^2 - |T_{\tilde{i}\tilde{f}}|^2$

With time-reversal invariance:

$$|T_{if}|^2 - |T_{\tilde{i}\tilde{f}}|^2 = 2\mathcal{I}(T_{if}\, a_{fi}) - |a_{if}|^2$$

[1] A. De Rujula, J. M. Kaplan, and E. De Rafael, Nucl. Phys. B35, 365 (1971)

Analyzing Power

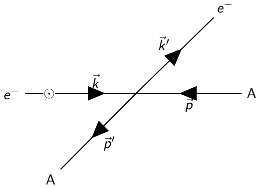

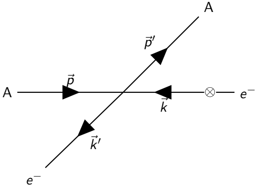

$$\mathcal{A}_n \equiv \frac{N_\uparrow - N_\downarrow}{N_\uparrow + N_\downarrow} = \frac{|T_\uparrow(\vec{k}, \vec{k}')|^2 - |T_\downarrow(\vec{k}, \vec{k}')|^2}{|T_\uparrow(\vec{k}, \vec{k}')|^2 + |T_\downarrow(\vec{k}, \vec{k}')|^2}$$

$$T_\downarrow(\vec{k}, \vec{k}') = e^{i\pi} T_\downarrow(-\vec{k}, -\vec{k}')$$

Let $T_{if} = T_\uparrow(\vec{k}, \vec{k}')$, apply time-reversal invariance:

$$\mathcal{A}_n \approx \frac{|T_\uparrow(\vec{k}, \vec{k}')|^2 - |T_\downarrow(-\vec{k}, -\vec{k}')|^2}{2|T_\uparrow(\vec{k}, \vec{k}')|^2} = \frac{|T_{if}|^2 - |T_{\tilde{i}\tilde{f}}|^2}{2|T_{if}|^2}$$

PREX-I Result

PREX-I PRL 109, 192501 (2012)

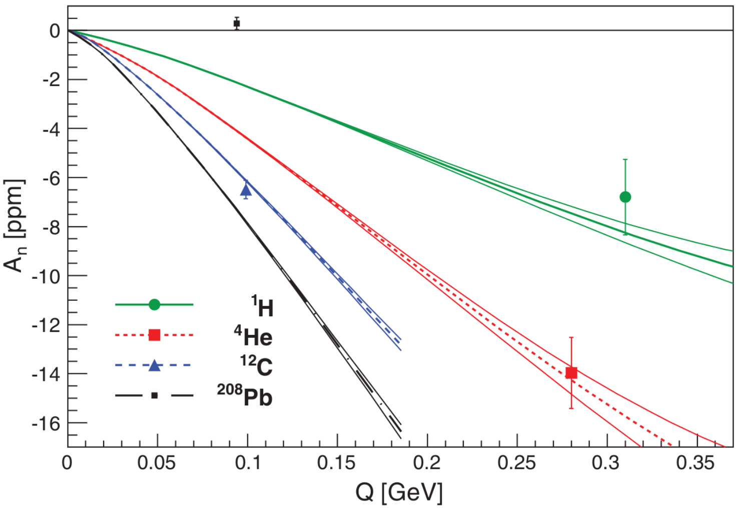

- Theoretical predictions match A_n measurements of light nuclei
- To everyone's surprise, A_n for Pb208 was measured to be 0

Phenomenological Fit

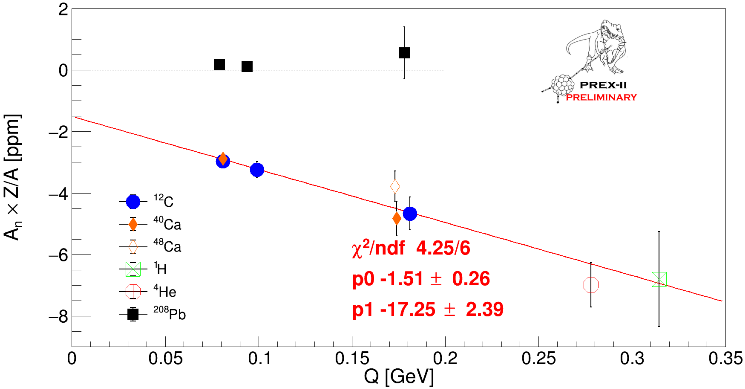

- For light nuclei, the linear fit of $A_n \times Z/A$ vs Q looks good
- Observe that it has a non-zero offset

Collimator Power

- Collimator is key component in these experiments, we need to make sure radiation deposit on collimator is under control
- The radiation power on collimator tells us the quality of target

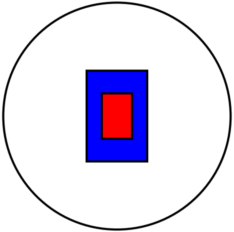

t_1 (mm)	t_2 (mm)	Power/Current (W/μA)
0.55	0.550	52.6172
0.45	0.583	53.4176
0.35	0.617	56.2972
0.25	0.650	58.7556
0.15	0.683	62.6694
0.05	0.717	66.8324

Collimator Power

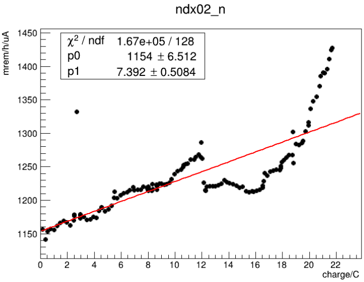

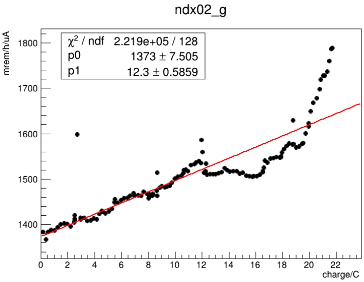

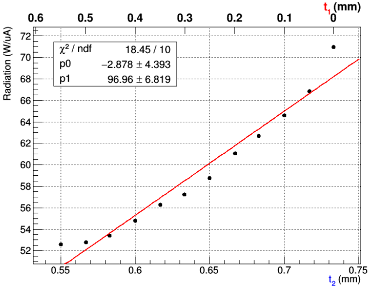

- Simulation result is consistent with experimental data: radiation increases along charge accumulation (target degradation)

All Hall A Measurements

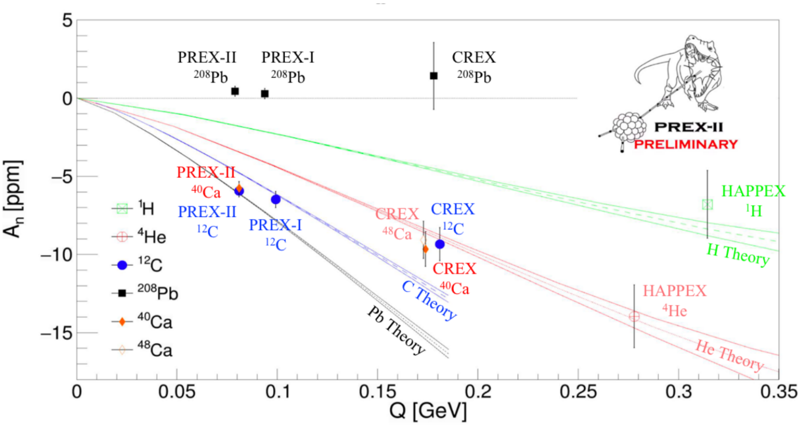

- A_n for Pb208 was found to be 0 at three different Q values
- For light nuclei, theoretical calculations follow the observed experimental measurements and trends

FFs

$$G_{E,M}^{p,\gamma} = \frac{2}{3} G_{E,M}^{u} - \frac{1}{3} G_{E,M}^{d} - \frac{1}{3} G_{E,M}^{s}$$
$$G_{E,M}^{n,\gamma} = \frac{2}{3} G_{E,M}^{d} - \frac{1}{3} G_{E,M}^{u} - \frac{1}{3} G_{E,M}^{s}$$
$$G_{E,M}^{n,Z^0} = \left(\frac{1}{4} - \sin^2\theta_W\right) G_{E,M}^{u} + \left(-\frac{1}{4} + \frac{1}{3}\sin^2\theta_W\right) \times \left(G_{E,M}^{d} + G_{E,M}^{s}\right)$$

Radius

$$R_n - R_p = \left[1 + \frac{ZQ_p}{NQ_n}\right](R_{wk} - R_{ch})$$

$$R_{ch} = 5.503 \text{ fm}$$

$$R_p = \sqrt{R_{ch}^2 - r_p^2} = 5.432 \text{ fm}$$

$$R_n - R_p = 0.278 \pm 0.078 \text{ fm}$$

Two-Parameter Fermi Function

$$\rho_w(r,c,a) = \rho_w^0 \frac{\sinh(c/a)}{\cosh(r/a) + \cosh(c/a)}$$

$$\rho_w^0 = \frac{3Q_w}{4\pi c(c^2 + \pi^2 a^2)}$$

$$R_w^2 = \frac{1}{Q_w}\int r^2 \rho_w(r) d^3 r = \frac{3}{5}c^2 + \frac{7}{5}(\pi a)^2$$

$$\rho_w^0 = \frac{27 Q_w}{4\pi(5R_w^2 - 4\pi^2 a^2)\sqrt{15 R_w^2 - 21\pi^2 a^2}}$$

$$R_w = 5.795 \pm 0.082 \text{ fm}$$

$$a = 0.605 \pm 0.025 \text{ fm from theory}$$

$$Q_w = NQ_w^n + ZQ_w^p = -118.78$$

$$\rho_w^0 = 0.080 \pm 0.004 \text{ fm}^{-3}$$

$$\rho_b^0 = \frac{-\rho_w^0}{q_n} + \left(1 - \frac{q_p}{q_n}\right)\rho_c^0$$

Systematic Uncertainties

Collimators

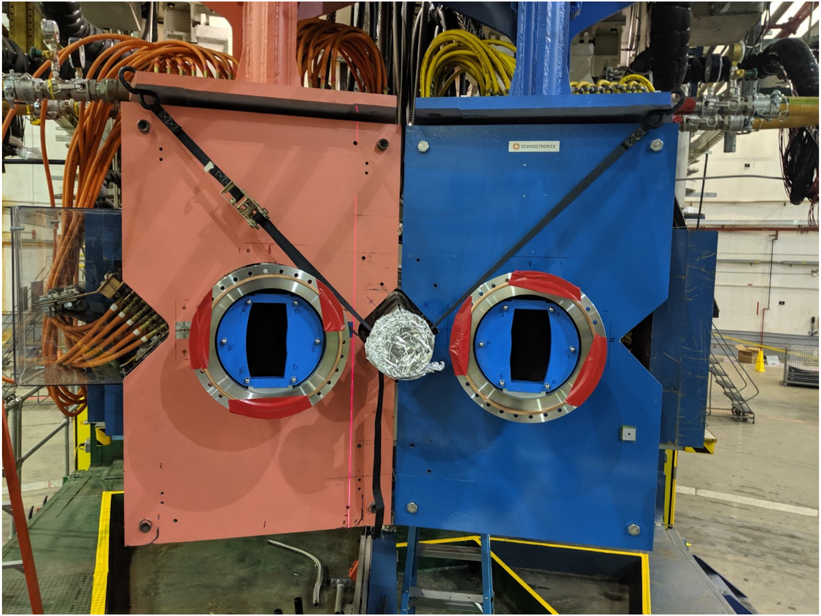

Carbon Contamination in Pb Target

$$\mathcal{A}_{\text{PV}} = \frac{\mathcal{A}_{\text{cor}}/\mathcal{P} - \sum_i \mathcal{A}_i \mathbf{f_i}}{1 - \sum_i \mathbf{f_i}}$$

Why D-Pb-D sandwich target?

- Lead has low melting point, and low thermal conductivity
- Diamond foils have excellent thermal conductivity
- Carbon background is clean

- The largest dilution: $f_c = (6.3 \pm 0.5)\%$
- Asymmetry correction: $\Delta\mathcal{A} = (0.7 \pm 1.4)$ ppb

Acceptance Function

$$\langle \mathcal{A} \rangle = \frac{\int d\theta \sin\theta \mathcal{A}(\theta) \frac{d\sigma}{d\Omega} \epsilon(\theta)}{\int d\theta \sin\theta \frac{d\sigma}{d\Omega} \epsilon(\theta)}$$

- The PREX-II/CREX experiments measure the average asymmetry over the spectrometer scattering angle acceptance
- An acceptance function is needed to connect our measurement with theoretical models
- The acceptance function is extracted from simulations

CREX Acceptance Fucntion: How Do We Know the Simulation is Correct

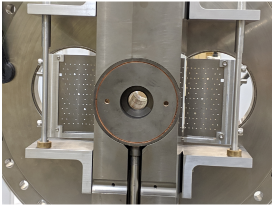

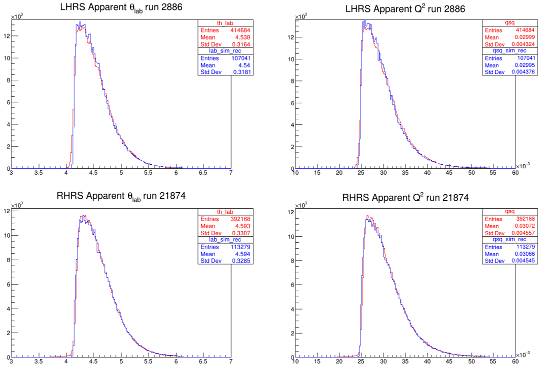

- There are sieve planes in front of the septum for track reconstruction
- By scanning through different parameters, we can identify the best model

CREX Acceptance Function: Result

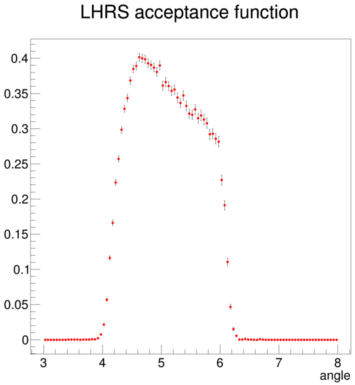

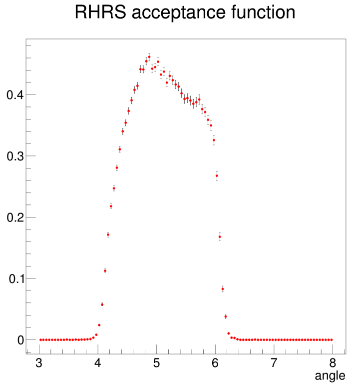

- LHRS (RHRS): Left (Right)-HRS
- The acceptance functions between the two arms are not exactly the same